

# In vitro analysis of metabolites from the untreated tissue of *Torpedo californica* electric organ by mid-infrared laser ablation electrospray ionization mass spectrometry

Prabhakar Sripadi · Javad Nazarian ·  
Yetrib Hathout · Eric P. Hoffman ·  
Akos Vertes

Received: 7 September 2008 / Accepted: 1 December 2008 / Published online: 14 December 2008  
© Springer Science+Business Media, LLC 2008

**Abstract** The neuromuscular junction (NMJ), where a motor neuron intercepts and activates a muscle fiber, is a highly versatile and complex subcellular region. Genomic and proteomic approaches using the large (>1 kg) electric organ of *Torpedo californica* have helped advancing our understanding of this minute (30–50 μm) electric synapse. However, the majority of these studies have focused on mRNA and proteins, therefore neglecting small signaling molecules involved in muscle-nerve ‘dialogue’. We developed a novel technique, mid-infrared laser ablation electrospray ionization (LAESI) mass spectrometry (MS), with the potential of detecting a diversity of small signaling molecules in vitro. LAESI uses the native water in the tissue as the matrix to couple the laser pulse energy into the target for the ablation process and enables its direct analysis essentially without sample preparation. Here, we report the detection of metabolites from the untreated frozen tissue of the *Torpedo* electric organ with LAESI MS at atmospheric pressure. A total of 24 metabolites were identified by accurate mass measurements, natural isotope patterns, and tandem mass spectrometry. Most of the identified metabolites were related to the cholinergic function of the electric synapse (acetylcholine and

choline), fatty acid metabolism and acetyl transfer (carnitine and acetylcarnitine), the mitigation of osmotic stress (betaine and trimethylamine N-oxide), and energy production (creatine and creatinine). The biosynthetic precursors of these metabolites and their expected degradation products were also detected indicating that LAESI MS is well suited for tissue metabolomics with the ultimate goal of imaging and in vivo studies.

**Keywords** *Torpedo californica* · Electric organ · Neuromuscular junction · Metabolites · Osmolytes · Metabolomics · Quantitation · Laser ablation · Electrospray ionization · LAESI · Collision activated dissociation

## 1 Introduction

Neuromuscular junctions have evolved to become specialized subcellular regions expressing unique molecular components. In response to electrical inputs from nerve and other yet unknown factors, myonuclei located directly beneath NMJs express a unique subset of genes generating what is known as subsynaptic myonuclear domains (Allen et al. 1999; Rossi et al. 2000). Such localized gene expression domains are essential for the initiation, maturation, and maintenance of synaptic scaffolding (Nazarian et al. 2005; Sanes and Lichtman 1999, 2001). Pruning for example, is a postnatal process by which a multi-innervated muscle dissociates from all but one motoneuron. Cellular and molecular mechanisms involved in pruning are of great interest and largely unknown mainly due to the limited ability of studying such interactions in vivo (Keller-Peck et al. 2001; Walsh and Lichtman 2003; Zito 2003). Molecules involved in the pruning process could include small

**Electronic supplementary material** The online version of this article (doi:10.1007/s11306-008-0147-x) contains supplementary material, which is available to authorized users.

P. Sripadi · A. Vertes (✉)  
Department of Chemistry, W. M. Keck Institute for Proteomics  
Technology and Applications, George Washington University,  
Washington 20052, USA  
e-mail: vertes@gwu.edu

J. Nazarian · Y. Hathout · E. P. Hoffman  
Research Center for Genetic Medicine, Children’s National  
Medical Center, Washington 20010, USA

peptides or metabolites as well as large proteins generated by any of the three cell types present at the NMJ; the muscle fiber, Schwann cells, and the motoneuron (Gillingwater and Ribchester 2003; Keller-Peck et al. 2001; Walsh and Lichtman 2003; Zito 2003). Certain species, such as electric fish, have developed whole organs from the specialized NMJ capable of generating up to 600 V of electricity (Kent 1992). The electric organ of *Torpedo californica* has been intensely studied as a model for understanding the minute electric synapses. These studies have resulted in the identification of major macromolecular components of the NMJ such as agrin and acetylcholine receptors (AChRs) (Kistler and Stroud 1981; Kistler et al. 1982; Mitra et al. 1989). Our objective was to develop novel methodologies to expand our understanding of the NMJ by defining the metabolome profile of the electric organ and muscle tissue in vitro with potential for in vivo studies.

In recent decades, rapidly expanding advances in genomic, proteomic, and metabolomic technologies have prepared the ground for an integrated understanding of living organisms and processes in cell biology (Bino et al. 2004; Dettmer et al. 2007; Vekey et al. 2008). Genomic studies map out the nucleic acid blueprint of an organism, whereas proteomics explores the translation of nucleic acids as peptides and proteins, hence reflecting important clues with regards to the physiological state of a cell or an organism. Metabolomic studies reveal the chemical signature of cellular processes specific to the functioning of the tissue. While genomics and proteomics have witnessed significant technological strides, tools for the comprehensive examination of the metabolome are slowly emerging. Metabolomic studies aim at the extensive qualitative and quantitative analysis of a wide array of metabolites in biological samples. Currently, two complementary approaches are used for metabolomic investigations: metabolic profiling and metabolic finger printing (Dettmer et al. 2007). Metabolic profiling focuses on the analysis of a group of metabolites, and the results are used to build databases that can be integrated with pathway maps that enhance biological understanding. In the metabolic fingerprinting the focus is on the pattern of metabolites rather than identifying each observed metabolite. Because metabolites are small molecules of diverse physicochemical properties and with different abundances, comprehensive metabolomics investigations usually require a number of different protocols targeting individual metabolites. It is generally accepted that a single analytical technique does not generate sufficient insight into the metabolome; rather multiple methodologies are needed for a comprehensive study (Bino et al. 2004; Dettmer et al. 2007; Mashego et al. 2007).

Numerous analytical platforms have been used towards metabolomic applications. Typical analytical techniques include: infrared (IR) spectroscopy, nuclear magnetic

resonance (NMR), and mass spectrometry (MS). In recent years MS has become an important tool for metabolomic applications because of its high molecular specificity, high sensitivity (low-detection limits), high throughput capabilities and its compatibility with separation techniques such as gas chromatography (GC), liquid chromatography (LC), and capillary electrophoresis (CE).

Apart from the detection methods, the analysis of metabolites requires special approaches for sample preparation. Rapid degradation of metabolites following an autopsy or the collection of a biopsy sample further complicates thorough metabolomic analysis. Earlier mass spectrometric methods involved laborious extraction and derivatization steps prior to analysis, especially when using the GC-MS method. General sample preparation protocols included liquid-liquid extraction or solid phase extraction of the metabolites followed by MS and tandem MS analysis. By using soft ionization methods, such as electrospray ionization (ESI) and matrix-assisted laser desorption ionization (MALDI), many polar metabolites could be analyzed avoiding the derivatization step. Conventional MALDI analysis, however, included the additional steps of mixing a suitable matrix, such as  $\alpha$ -cyano-hydroxycinnamic acid, to the sample extracts and inserting the sample into vacuum. Ideally, the samples must be preserved in their native state with preferably no or minimal interference from the analysis. For example, in UV-MALDI imaging experiments, tissue analysis is carried out by uniformly covering the tissue sections with a matrix without significantly altering the molecular distributions. These delicate and laborious procedures considerably restrict the choice of samples and exclude the possibility of in vivo studies.

To overcome these problems, a number of ambient ion sources, such as direct analysis in real time (DART), (Cody et al. 2005; Pierce et al. 2007) desorption electrospray ionization (DESI), (Takats et al. 2004) atmospheric pressure infrared MALDI (AP IR-MALDI), (Li et al. 2007, 2008) and laser ablation electrospray ionization (LAESI) (Nemes and Vertes 2007; Nemes et al. 2008; Vertes et al. 2008) have been developed. AP IR-MALDI and LAESI have proved particularly useful in targeting diverse primary and secondary plant metabolites without sample preparation. The unique advantage of the AP IR-MALDI and LAESI techniques is the use of the native water in the sample as the matrix. This enables the direct analysis of biological tissue because most of their cells contain 60–90% water. Although these two techniques have been successfully used to analyze metabolites in plants and in human blood (Nemes and Vertes 2007) and urine (Shrestha et al. 2008) samples, they have not been described for animal tissues.

Here we report a novel mass spectrometric approach for the direct detection of metabolites in the *Torpedo californica* electric organ by LAESI methodology. We show that

the native water can be used as an efficient matrix for mid-IR laser ablation followed by electrospray postionization for positive ion generation. We demonstrate that LAESI enables the direct analysis of electric organ tissue with minimal (30-s) sample handling. We report the identification of numerous metabolites related to the synaptic cleft and other important biosynthetic precursors/products in the electric organ.

## 2 Materials and methods

### 2.1 Materials

The electric organ and tail muscle tissues of *Torpedo californica* (Pacific electric ray) were obtained from Aquatic Research Consultants (San Pedro, CA) and stored at  $-80^{\circ}\text{C}$ . The tissue was used as received without any treatment. To test the integrity of the tissue, immunohistochemistry assays were performed on the sections using bungarotoxin that stained acetylcholine receptors. An ample staining indicated the integrity of the membranes and tissue preservation (see Fig. 1).

All solvents were HPLC grade from Acros Organics (Geel, Belgium). Ultrapure  $\alpha$ -cyano-4-hydroxycinnamic acid (CHCA) and 2,5-dihydroxybenzoic acid (DHB) were obtained from Protea Biosciences, Inc. (Morgantown, WV). The glacial acetic acid was purchased from Fluka (Munich, Germany). Standard samples for betaine, carnitine, choline, and  $\text{d}_9$ -choline (*N,N,N*-trimethyl- $\text{d}_9$ ) were commercially available (Sigma-Aldrich, St. Louis, MO) as their hydrochloride salts and were used as received. Acetyl- $\text{d}_3$ -carnitine was purchased from Cambridge Isotope

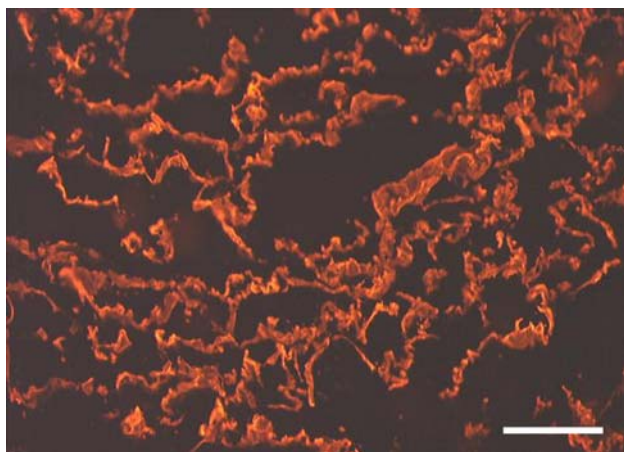


**Fig. 1** *Torpedo californica* electric organ was dissected (20  $\mu\text{m}$ ) and stained with bungarotoxin which binds to alpha-acetylcholine receptor subunits. Extensive staining showed that postsynaptic membrane was indeed intact and that this electric organ represented a giant NMJ. Scale bar = 30  $\mu\text{m}$

Laboratories, Inc. (Andover, MA) as its hydrochloride salt. A manual microtome (Colorado Scientific Company, Denver, CO) was used for sectioning the frozen electric organ tissue. The  $\sim 200$   $\mu\text{m}$ -thick sections were quickly transferred onto a microscope slide and directly used for the analysis.

### 2.2 Laser ablation electrospray ionization

Laser ablation was performed by a mid-IR laser system. An optical parametric oscillator (OPO) (Opolette 100, Oportek, Carlsbad, CA) converted the output of a 100-Hz repetition rate Nd:YAG laser to mid-IR pulses of 5-ns duration at 2,940-nm wavelength. Beam steering and focusing were accomplished by gold coated mirrors (PF10-03-M01, Thorlabs, Newton, NJ) and a 150 mm focal length  $\text{CaF}_2$  lens (Infrared Optical Products, Farmingdale, NY), respectively. At  $\sim 5$ –6 mm downstream from the tip of the spray capillary, the laser beam with average output energy of 0.3 mJ/pulse was used to ablate the tissue sample at  $90^{\circ}$  incidence angle. Based on the burn pattern it produced on photographic paper, optical microscopy indicated that the laser spot size had  $\sim 300$   $\mu\text{m}$  average diameter.

The electrospray system was similar to the one described in a recent report from our laboratory (Nemes et al. 2008). Briefly, a home-built electrospray system with a low-noise syringe pump (Physio 22, Harvard Apparatus, Holliston, MA) was used to feed the 50% methanol solution containing 0.1% (v/v) acetic acid through a stainless steel capillary (130  $\mu\text{m}$  i.d. and 260  $\mu\text{m}$  o.d.) with a blunt tip (90531, Hamilton Co.). A stable high voltage (2,600 V) was generated by a regulated power supply (PS350, Stanford Research Systems, Inc., Sunnyvale, CA) and was directly applied to the emitter. The orifice of the sampling cone was lined up on-axis with the electrospray emitter at a distance of 12 mm from its tip. The microscope slide with the sample was held at ambient temperature and was positioned 18 mm below the spray axis. The microscope slide was mounted on a computer-controlled stepper motor-driven three-axis precision flexure stage (Nanomax TS, Thorlabs, Newton, NY) for rastering and geometry optimization.

The home-built LAESI ion source was mounted on a Q-TOF Premier mass spectrometer (Waters, Milford, MA). Full scan mass spectra were recorded over the mass range of  $m/z$  50–2,000 using a time-of-flight (TOF) analyzer at a resolution of 8,000 (FWHM). Collision activated dissociation (CAD) spectra were recorded by selecting the precursor ion using the quadrupole analyzer (transmission window 2 Da) and the product ions were resolved by the TOF analyzer. Argon was used as the collision gas at a typical collision cell pressure of  $4 \times 10^{-3}$  mbar, and a collision energy set between 5 and 25 eV. Accurate masses were determined using the internal standard method.

Glycine, methionine, *N*-acetyl phenylalanine, and leucine enkephalin were dissolved at the appropriate concentrations (50–200  $\mu\text{M}$ ) in the electrospray solution and used as internal standards.

### 2.3 Quantitation by LAESI

For external calibration aqueous stock solutions with 1 M concentration of betaine, carnitine, and choline were prepared. Standard solutions were obtained by making appropriate dilutions of the stock solutions with deionized water. Except for the reduced 20-Hz laser repetition rate, the LAESI experimental conditions for quantitative analysis were similar to those used for the qualitative analysis. All experiments were performed in triplicates. To record a LAESI spectrum, 10  $\mu\text{l}$  of the standard solution was placed on a microscope slide and exposed to the laser pulses. Counts of the quasi-molecular ions, obtained from the 5-scan average spectrum, were measured to generate the calibration graphs. The LAESI spectra of *Torpedo* electric organ were recorded at identical conditions and the metabolites of interest were quantified by using the calibration curves obtained for the corresponding standards. In the ion suppression experiments, the  $\text{d}_9$ -choline was added to the tissue freeze/thaw solution.

For internal calibration the tissue (1–2 g) was spiked with appropriate volumes of deuterium labeled compound (100 mM stock solution of  $\text{d}_9$ -choline and acetyl- $\text{d}_3$ -carnitine) to get different final concentrations of the spiked chemical in the tissue. The tissue was then frozen in liquid nitrogen and pulverized using a mortar and pestle. The grinding process was repeated 3–4 times to get a homogenous tissue paste. A small portion of the tissue paste was loaded onto a microscope slide for LAESI analysis in triplicates.

### 2.4 UV-MALDI

MALDI spectra were recorded on a Kratos Axima CRF TOF-MS (Kratos Analytical, Manchester, UK) fitted with a nitrogen laser ( $\lambda_{\text{max}}$ , 337-nm; pulse width, 3 ns), using pulsed extraction and curved reflectron for high resolution, and operating in positive ion mode. CHCA or DHB (10 mg/ml) in acetonitrile:0.1% aqueous TFA (50:50, v/v) was used as the matrix solution. A thin slice of tissue was placed on the stainless steel target and allowed to dry under ambient conditions. Then 2  $\mu\text{l}$  of the matrix solution loaded on the sample and dried under ambient conditions. The laser power was optimized to the matrix used (60 for CHCA and 100 for DHB).

### 2.5 ESI analysis

Approximately 250 mg of tissue was transferred into an eppendorf tube and extracted with 500  $\mu\text{l}$  water by a

freeze/thaw process (five cycles) between  $-80^\circ\text{C}$  and room temperature. The contents were centrifuged at 10,000 rpm for 2 min. The water layer was transferred into a fresh tube and diluted with equal volume of acetonitrile with 0.1% formic acid. The solution was then infused into our ESI source at a flow rate of 300 nl/min. The mass spectrometer conditions were identical to those used for the LAESI experiments.

## 3 Results and discussion

Frozen *Torpedo* electric organ was sectioned ( $\sim 200 \mu\text{m}$ -thick) and placed on microscope slide and analyzed by LAESI as described in the [Materials and Methods](#) section. The positive ion LAESI mass spectra obtained from the *Torpedo* electric organ tissue exhibited exclusively singly charged ions with significant abundances (Fig. 2). Stringent ion identification included structure elucidation based on accurate mass measurements, isotope distribution patterns and, in some cases, tandem MS analysis (CAD experiments). A total of 24 metabolites were identified and these are listed in Table 1 with their theoretical and observed molecular masses, their specific fragment ions as well as their biological activity. This list also includes some detected metabolite ions tentatively assigned based on their accurate mass measurements together with biosynthetic pathway information for the identified molecules.

An important advantage of coupling the LAESI ion source to a Q-TOF mass spectrometer is the high resolution capability of the TOF analyzer, which enables the

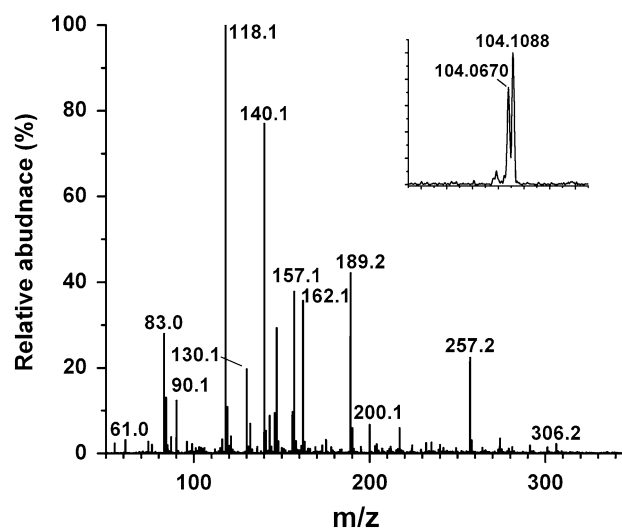


**Fig. 2** Typical positive ion LAESI spectrum directly from *Torpedo* electric organ tissue. Inset shows the expanded spectrum with peaks of two different metabolites, dimethylglycine and/or GABA with  $m/z$  104.0670 and choline with  $m/z$  104.1088, of the same nominal  $m/z$  104

**Table 1** Peak assignments for the ions observed in the LAESI spectra of *Torpedo* electric organ tissue

Metabolite	Chemical formula	Monoisotopic mass	Measured mass ( <i>m/z</i> )	$\Delta m$ (mDa)	MS/MS ions	Biological activity
Trimethylamine	C <sub>3</sub> H <sub>9</sub> N	60.0813(+H)	60.0870	5.7		Decomposition product
Urea	CH <sub>4</sub> N <sub>2</sub> O	61.0402(+H)	61.0409	0.7	44 <sup>a</sup>	Urea cycle, osmotic balance
		83.0197(+Na)	83.0221	2.4		
		121.0726(2M + H)	121.0777	5.1		
		143.0545(2M + Na)	134.0543	-0.2		
Tetramethylammonium ion	C <sub>4</sub> H <sub>11</sub> N	74.0970	74.0963	-0.7	58, 59	Blocking of sodium channels
Trimethylamine <i>N</i> -oxide or methyl ethanolamine	C <sub>3</sub> H <sub>9</sub> NO	76.0762(+H)	76.0797	3.5		Organic osmolyte Choline biosynthesis
Tetrahydropyridine or 2,3-dihydro, 1-methyl pyrrole or Cycloalkenyl amine	C <sub>5</sub> H <sub>9</sub> N	84.0813(+H)	84.0816	0.3		
<i>N</i> -Methyl glycine or $\beta$ -Alanine	C <sub>3</sub> H <sub>7</sub> NO <sub>2</sub>	90.0555(+H)	90.0580	2.5		Creatine metabolite Inhibitory neurotransmitter
Betaine aldehyde	C <sub>5</sub> H <sub>12</sub> NO	102.0919	102.0929	1	59, 74, 85, 85 <sup>a</sup>	Choline metabolite/betaine precursor
Dimethyl glycine or GABA	C <sub>4</sub> H <sub>9</sub> NO <sub>2</sub>	104.0712 (+H)	104.0670	-4.2		Betaine metabolite Inhibitory neurotransmitter
Choline	C <sub>5</sub> H <sub>14</sub> NO	104.1075	104.1088	1.3	60, 58 <sup>c</sup>	Precursor for acetylcholine
2-amino 4(1H)pyri-midinone or 4-amino 2(1H)pyrimi-dinone	C <sub>4</sub> H <sub>9</sub> NO <sub>2</sub>	112.0511(+H)	112.0554	4.3		Antagonists of the neurotransmitters
Creatinine	C <sub>4</sub> H <sub>7</sub> N <sub>3</sub> O	114.0667(+H)	114.0647	-2	86 <sup>a</sup>	Breakdown product of creatine phosphate in muscle
		136.0487(+Na)	136.0532	4.5		
Proline	C <sub>5</sub> H <sub>9</sub> NO <sub>2</sub>	116.0712(+H)	116.0753	4.1	70 <sup>b</sup>	Non-essential amino acid
		138.0531(+Na)	138.0561	3		
Betaine	C <sub>5</sub> H <sub>11</sub> NO <sub>2</sub>	118.0868(+H)	118.0826	-4.2	58, 59 <sup>a</sup>	Organic osmolyte
		140.0687(+Na)	140.0719	3.2		
		156.0427(+K)	156.0453	2.6		
		257.1477(2M + Na)	257.1492	1.5		
Pipecolic acid	C <sub>6</sub> H <sub>11</sub> NO <sub>2</sub>	130.0868 (+H)	130.0894	2.6	84 <sup>a</sup>	Intermediate in the catabolism of lysine
Creatine	C <sub>4</sub> H <sub>9</sub> N <sub>3</sub> O <sub>2</sub>	132.0773 (+H)	132.0786	1.3	90 <sup>a</sup>	Energy supply to muscle and nerve cells
		154.0592 (+Na)	154.0543	-4.9		
Acetylcholine	C <sub>7</sub> H <sub>16</sub> NO <sub>2</sub>	146.1181	146.1192	1.1	60, 87 <sup>b</sup>	Neurotransmitter
Lysine	C <sub>6</sub> H <sub>14</sub> N <sub>2</sub> O <sub>2</sub>	147.1134 (+H)	147.1152	1.8	84, 130 <sup>b</sup>	Essential amino acid, metabolizes to give acetyl-CoA
Glutamine	C <sub>5</sub> H <sub>10</sub> N <sub>2</sub> O <sub>3</sub>	147.0770 (+H)	147.0789	1.9	84, 130 <sup>b</sup>	Excretion of ammonia
Carnitine	C <sub>7</sub> H <sub>15</sub> NO <sub>3</sub>	162.1130 (+H)	162.1151	2.1	60, 85, 103 <sup>b</sup>	Fatty acid metabolism, acetyl transfer reactions
Phenylalanine	C <sub>9</sub> H <sub>11</sub> NO <sub>2</sub>	166.0868 (+H)	166.0918	5.0		Essential amino acid
Dimethyllysine	C <sub>8</sub> H <sub>18</sub> N <sub>2</sub> O <sub>2</sub>	175.1447 (+H)	175.1463	1.6		Intermediate for trimethyllysine
Trimethyllysine	C <sub>9</sub> H <sub>20</sub> N <sub>2</sub> O <sub>2</sub>	189.1603 (+H)	189.1589	-1.4	84, 130 <sup>d</sup>	Precursor for the biosynthesis of carnitine
Acetylcarnitine	C <sub>9</sub> H <sub>17</sub> NO <sub>4</sub>	204.1236 (+H)	204.1249	1.3	60, 85, 145 <sup>b</sup>	Acetyl source for biosynthesis
Butyryl-carnitine	C <sub>11</sub> H <sub>22</sub> NO <sub>4</sub>	232.1549	232.1504	-4.5	85, 173 <sup>d</sup>	Carnitine metabolite

<sup>a</sup> <http://www.massbank.jp> (Last Accessed on July 16, 2008)<sup>b</sup> NIST Mass Spectral Search Program for the NIST/EPA/NIH Mass Spectral Library, Version 2.0<sup>c</sup> Hanley et al. (2007)<sup>d</sup> Holm et al. (2003)

distinction between different metabolites with the same nominal mass. Examples of such metabolites are dimethylglycine and  $\gamma$ -aminobutyric acid (GABA,  $m/z$  104.0670) and choline ( $m/z$  104.1088) (see inset in Fig. 2). Based on the 42 mDa mass difference, choline can be clearly distinguished from dimethylglycine and  $\gamma$ -aminobutyric acid, while dimethylglycine and GABA, that are structural isomers, cannot be differentiated based solely on accurate mass analysis.

Typical tandem MS spectra for the primary ions  $m/z$  147 and 162 are shown in Figs. 3 and 4, respectively. To obtain a better CAD signal, especially for low abundance precursor ions, the quadrupole transmission window was set to 2 Da. The CAD spectrum recorded for  $m/z$  147 (Fig. 3) showed fragment ions at  $m/z$  84 and 130, which were characteristic to lysine/glutamine. However, due to the 2 Da transmission window the spectrum also included fragment ions  $m/z$  60 and 87 corresponding to acetylcholine ( $m/z$  146) that is 1 Da apart from lysine/glutamine. The CAD spectrum of carnitine ( $m/z$  162, Fig. 4), however, showed only the expected fragment ions.

Most of the identified metabolites described below in detail are polar compounds, expected to be present in the electric organ tissue.

### 3.1 Acetylcholine and choline

We readily identified the neurotransmitter acetylcholine (ACh) and its precursor choline directly from the *Torpedo* electric organ. Nerve endings of the *Torpedo* electric organ contain synaptic vesicles (30–120 nm in diameter) wherein the ACh is stored. Vesicles isolated from rested fish are

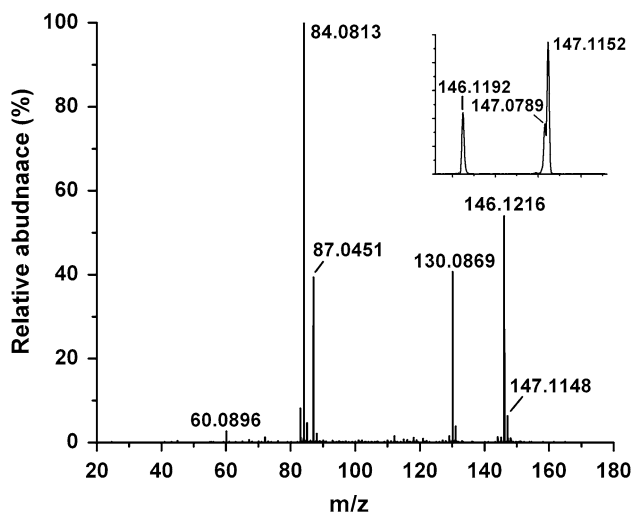


**Fig. 3** CAD tandem mass spectrum of nominal  $m/z$  147 ions corresponding to protonated lysine and glutamine and of  $m/z$  146 ion identified as acetylcholine directly from *Torpedo* electric organ tissue. In the inset the expanded LAESI spectrum shows the three parent peaks with their measured accurate masses

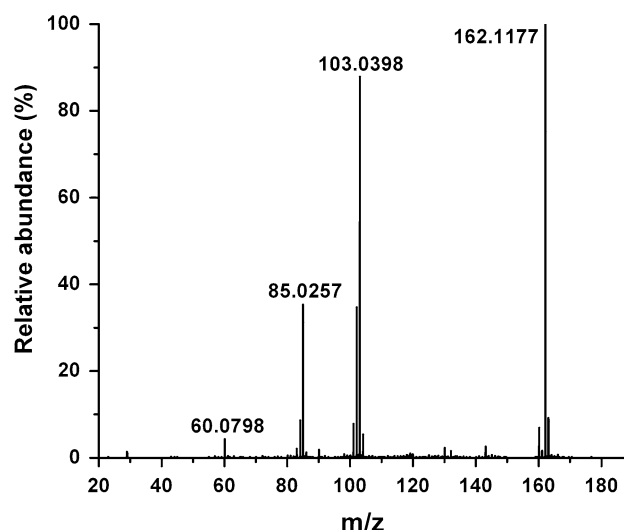


**Fig. 4** CAD tandem mass spectrum of protonated carnitine with nominal  $m/z$  162 produced by LAESI directly from *Torpedo* electric organ tissue

known to contain an average concentration of 0.6 M osmotically active ACh (Breer et al. 1978; Morris et al. 1965; Stadler and Fuldner 1980). According to Feldberg and Fessard, 40–100  $\mu\text{g}$  ACh can be extracted from 1 g of fresh *Torpedo* electric organ tissue (Feldberg and Fessard 1942). Based on our experience with tissue ablation, the laser removes up to 40  $\mu\text{m}$  material from a 300  $\mu\text{m}$  diameter spot. Thus the removed tissue volume is  $\sim 3$  nl and the corresponding mass is  $\sim 3$   $\mu\text{g}$ . This corresponds to an estimated 120–300 pg of ACh sampled by a laser pulse.

Terminal nerves of the electric organ of *Torpedo* are purely cholinergic forming synapses highly similar to vertebrate NMJs. ACh is released from synaptic vesicles into the synaptic cleft upon nerve stimulation by exocytosis. The released ACh binds to acetylcholine receptors on the postsynaptic muscle and causes an increase in the permeability of ligand-gated sodium ion channels. ACh is rapidly broken down to choline in the synaptic cleft by the enzyme acetylcholine esterase (Fig. 5). The neurotransmitter, ACh, is synthesized in the cytoplasm by the transfer of acetyl group from acetyl-CoA to choline using the enzyme choline acetyltransferase and then the ACh is transported into the vesicles for reuse (Anderson et al. 1982). The biosynthesis of choline is well-known which mainly involves three pathways, one of which is from glycine via methylethanolamine and dimethylethanolamine. Here we detect the ion  $m/z$  76 whose elemental composition corresponds to methylethanolamine, however, it also matches with trimethylamine *N*-oxide. The detection and identification of ACh confirmed the validity of our technique. Therefore, we expanded the analysis of the spectra to identify known and unknown metabolites integral to the electric organ.

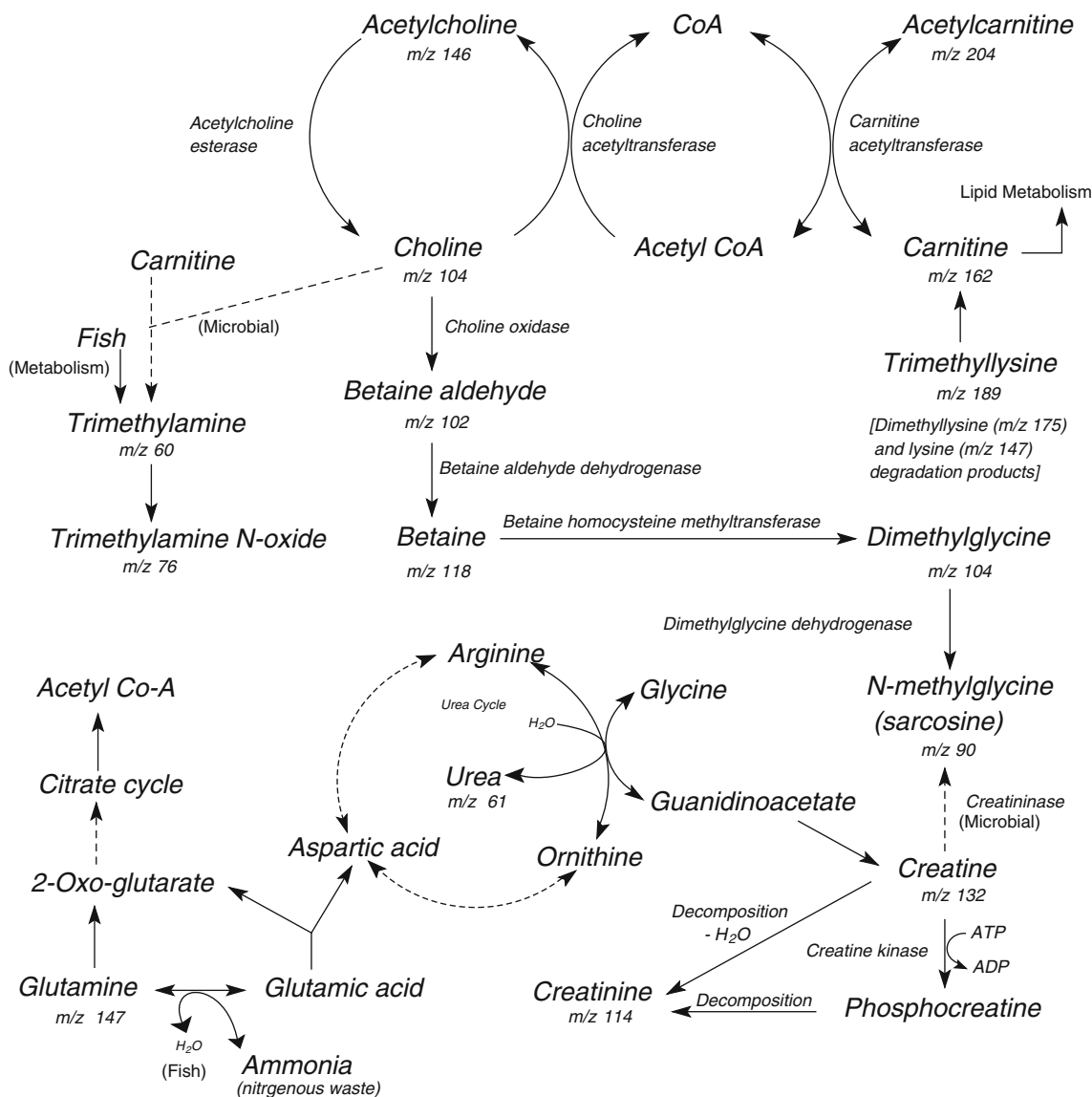


**Fig. 5** Metabolites identified in this study are designated by their nominal  $m/z$  values. Related enzymes in the metabolomic/biosynthetic pathways of betaine, choline, creatine, carnitine, and urea are shown in italics

### 3.2 Betaine and its metabolites

Betaine was also detected among metabolites present in the electric organ. Although betaine is well-known to be present in the muscles of elasmobranchs (Shewan 1953; Treberg et al. 2006), to the best of our knowledge the presence of glycine betaine in the *Torpedo* electric organ has not been reported earlier. Based on the LAESI spectra obtained, glycine betaine appears to be the most abundant metabolite in the *Torpedo* electric organ (see the  $MH^+$  ion peak at  $m/z$  118 in Fig. 2). Betaines are a class of naturally occurring compounds that have an important role in osmotic stress and high salinity resistance in a variety of organisms including bacteria, algae, mammals, and plants. In some cases betaines accumulate up to a concentration of

1 M inside cells subjected to osmotic upshock (Caldas et al. 1999) facilitating protein and membrane integrity against the adverse destabilizing effects of inorganic ions. Recently, Hayashi et al. studied the dielectric properties of glycine betaine and urea by dielectric spectroscopy (Hayashi et al. 2007). They found that hydration of betaine was much higher than urea, and hence betaines play a critical role in the stabilization of native protein conformation. Glycine betaine is also a methyl donor of increasing significance (Park and Garrow 1999).

The biosynthesis of betaine is well established in animals and plants. The pathway includes the formation of glycine betaine from choline via betaine aldehyde (Fig. 5), and the glycine betaine leads to the metabolite dimethylglycine. We identified all of these compounds in the

*Torpedo* electric organ, which corroborated the described pathways of glycine betaine metabolism (Fig. 5). In addition, we have found tetramethylammonium ions in the tissue that have a similar function to betaines (Yancey et al. 1982) and are used for the blockage of sodium channels as well (Keynes et al. 1992; Woodhull 1973). There have been numerous reports on the characterization of betaines for plants using HPLC and tandem MS that include the extraction of sample, but the present approach represents a simple method for the analysis of these molecules directly from tissue (Colmer et al. 2000; Wood et al. 2002).

### 3.3 Carnitine, acetylcarnitine, and their biosynthesis

We also identified the presence of carnitine and acetylcarnitine in the electric organ tissue. Carnitine is an essential metabolite, which has a number of indispensable roles in intermediary metabolism. Carnitine is present in most animal species, plants, and micro-organisms. One of its vital roles is in the transport of activated long-chain fatty acids from the cytosol to the mitochondrial matrix, where  $\beta$ -oxidation takes place (McGarry and Brown 1997; Vaz et al. 2002; Vaz and Wanders 2002). Secondly, carnitine is involved in the transfer of the products of peroxisomal  $\beta$ -oxidation, including acetyl-CoA, to the mitochondria for CO<sub>2</sub> and H<sub>2</sub>O oxidation. (Jakobs and Wanders 1995; Verhoeven et al. 1998) Other functions of carnitine include modulation of the acyl-CoA/CoA ratio, storage of energy as acetylcarnitine (Brass 2002; McGarry and Brown 1997; Steiber et al. 2004) and the modulation of toxic effects of poorly metabolized acyl groups by excreting them as carnitine esters (Rebouche and Seim 1998).

Animal tissues contain relatively high amounts of carnitine, varying between 0.2 and 6  $\mu\text{mol/g}$  or 30–1,000  $\mu\text{g/g}$ , with the highest concentrations in heart and skeletal muscle (Vaz and Wanders 2002). Although animals obtain carnitine primarily from their diet, most mammals are capable of synthesizing carnitine endogenously. Most eukaryotes can synthesize this compound from trimethyllysine (Vaz et al. 2001). We also identified the biosynthetic precursor of carnitine, trimethyllysine in the *Torpedo* electric organ tissue. Free lysine and dimethyllysine are also identified, however, these cannot be precursors for the trimethyllysine because trimethyllysine is directly released from proteins by an enzymatic reaction (Bremer 1983). The free lysine and dimethyllysine could be formed by similar mechanisms yet to be determined.

We also identified acetylcarnitine in the tissue. It had carnitine and acetyl moieties with well-known neurobiological properties (Pettegrew et al. 2000). External acetate is the best substrate of ACh synthesis in the *Torpedo*

electric organ. Based on radiolabeled acetate experiments it was demonstrated that the acetate was incorporated into ACh, acetyl carnitine, and amino acids (aspartate, glutamate, and glutamine) (Corthay et al. 1985). The acetyl-CoA acts as substrate for choline acetyltransferase to produce ACh from choline. The acetyl moiety of acetylcarnitine can be used to maintain acetyl-CoA levels. The origin of acetyl groups in the acetyl-CoA, which is used for the synthesis of ACh, has been investigated in animal tissue by several groups. The role of acetylcarnitine in the synthesis of ACh, however, is yet to be resolved.

We also identified another carnitine metabolite, butyrylcarnitine. Both butyrylcarnitine and acetylcarnitine belong to group of acylcarnitines which have many neurobiological effects, including lipid metabolism, synaptic transmission of neurotransmitters and other potential molecular activity such as acylation of  $-\text{NH}_2$  and  $-\text{OH}$  functional groups and acting as molecular chaperones (Pettegrew et al. 2000). Determination of free carnitine and its esters in biological material is very important for clinical diagnosis also (Bhuiyan et al. 1992). A number of analytical procedures for qualitative and quantitative carnitine/acylcarnitine profiling are available today, but they include time consuming sample preparation methods (Ghoshal et al. 2005, Kamimori et al. 1994; Mardones et al. 1999), whereas the LAESI method enables high throughput analysis without tedious sample preparation steps.

### 3.4 Creatine and creatinine

Creatine, creatinine, and *N*-methylglycine (sarcosine) were also detected in the present study. The latter two could be formed as decomposition products from creatine. Creatine is another important nitrogenous organic molecule that helps to supply energy to muscle and nerve cells. We have previously shown the high abundance of creatine kinase (CK) in *Torpedo* electric organ (Nazarian et al. 2007). CK helps to maintain the necessary ATP levels in tissues with high energy demands by catalyzing the reversible transfer of a phosphoryl group between ATP and creatine. Creatine is also linked to the urea cycle via the intermediate guanidine acetate (Fig. 5). Detection of metabolites involved in urea cycle and their potential role is further described below.

### 3.5 Urea and glutamine

The presence of urea in the *Torpedo* electric organ tissue is clearly demonstrated by the *m/z* 61, 83, and 143 ions in the spectrum that correspond to quasimolecular urea ions,  $[\text{M} + \text{H}]^+$ ,  $[\text{M} + \text{Na}]^+$ , and  $[2 \text{M} + \text{Na}]^+$ , respectively. Urea is the major end product of nitrogen metabolism in



humans and mammals. Most of the nitrogenous waste comes from the breakdown and deamination of amino acids that result in the production of ammonia. The urea cycle describes the conversion of ammonia into urea. Aquatic animals, such as fish, remove waste nitrogen as ammonia that diffuses across the gills into the water (Randall and Ip 2006). It is known, however, that depending on the salinity of the water, fish can excrete urea via the urea cycle (Randall et al. 1989). Furthermore, the clasmobranchs (sharks and rays) synthesize and retain high concentrations of urea in their tissues for the purpose of maintaining an osmotic balance with the high salt concentration in sea water (Goldstein et al. 1968).

It was also interesting to find glutamine in the tissue. Glutamine can only be confirmed by high resolution data (see inset of Fig. 3), because glutamine and lysine are isobaric with theoretical masses 147.0770 and 147.1134, respectively, and both generate the same fragment ions in their CAD spectra ( $m/z$  84 and 130). Glutamine is one of the 20 amino acids generally present in animal proteins, and is involved in more metabolic processes than any other amino acid because of the two amino groups in it. In fish, glutamine is carried to a membrane in the gills near the surrounding water where a hydrolysis of the glutamine to glutamic acid releases the ammonia (Smutna et al. 2002). Glutamine is also indirectly linked to the urea cycle and the citrate cycle.

### 3.6 Trimethylamine and trimethylamine *N*-oxide

Trimethylamine, a decomposition product of plants and animals, and its oxidation product trimethylamine *N*-oxide (TMAO) were also detected in the electric organ tissue. TMAO belongs to the group of methylamines (organic osmolytes) that include betaine and sarcosine (Burg and Ferraris 2008; Yancey et al. 1982). The marine animals accumulate urea along with methylamines in a particular ratio to balance the high osmolality of sea water. There have been many analytical methods (GC, HPLC, NMR, and MS) developed for the detection and quantification of trimethylamine, because of its role in the evaluation of fish quality and diagnostics of human diseases (Bain et al. 2004). Recently, Johnson reported a flow injection ESI-MS/MS method for trimethylamine; however, the method included derivatization with ethyl bromoacetate (Johnson 2008). Here we demonstrated the LAESI analysis of these compounds directly from the tissue with straightforward extension to bodily fluids and without extraction or derivatization.

### 3.7 Quantitation of selected metabolites

Limited information is available on the metabolite concentrations in the electric organ tissue. For example, ACh

levels in synaptosomes were measured by a chemiluminescent method (Israel and Lesbats 1981). In clinical samples, plasma levels of carnitine are commonly determined by tandem MS (Vaz and Wanders 2002). Here we present the initial attempts to quantitate typical metabolites from the electric organ tissue by LAESI MS.

In an earlier report, the quantitation capabilities of LAESI MS were tested with standard solutions of verapamil and reserpine and it was demonstrated that the LAESI spectra provided linear response with a four-decade dynamic range (Nemes and Vertes 2007). Working with tissue samples presents three major challenges. First, laser ablation sampling might induce discrimination due to the difference in the volatility of various species; second, the ion suppression effect in ESI can skew the measured abundances; and finally, spectral interferences might take place because of the complex tissue matrix.

Nevertheless, we performed quantitation of typical metabolites identified in electric organ tissue, namely betaine, carnitine, and choline, using external calibration standards. Within the used concentration ranges, the LAESI spectra of the carnitine and choline standards exclusively showed the corresponding protonated molecule at  $m/z$  162 and 104, respectively. The spectrum of betaine, especially at higher concentrations, showed monomeric and dimeric quasi-molecular ions ( $m/z$  118, 140, 156 and 257, see Table 1 for details). The calibration curves (data not shown) were generated by plotting the logarithmic values of the ion counts for the quasi-molecular ion measured in the average spectrum of five scans against the component concentrations. The concentrations of the selected metabolites in the electric organ tissue were calculated from the standard calibration graphs assuming a tissue density close to 1 g/cm<sup>3</sup>. The measured tissue concentrations were  $0.89 \pm 0.02$  mg/g for betaine,  $8.3 \pm 0.4$   $\mu$ g/g for carnitine, and  $0.57 \pm 0.08$   $\mu$ g/g for choline. Based on the structural similarity between choline and acetylcholine, we also estimated the concentration of acetylcholine using the calibration curve obtained for choline. The tissue concentration of acetylcholine thus measured was  $1.6 \pm 0.1$   $\mu$ g/g, a value significantly below the figures established in the literature (Feldberg and Fessard 1942).

To explore the origin of this discrepancy, isotope labeling experiments were conducted. First, use of  $d_9$ -choline in ESI solution was verified, where solutions with equal concentrations of choline and  $d_9$ -choline were used as the sample ablated by the laser and in the electrospray solutions, respectively. The labeled compound from the electrospray appeared in the spectra at  $\sim 30$ -times higher abundances (data not shown). These results are obvious by the fact that the sample plume from laser ablation will only a small fraction in the mist of droplets originated from ESI solution. For the same reason,

presence of  $d_9$ -choline in ESI solution will not help to predict actual ion suppression effects from sample matrix during laser ablation. In fact, ion suppression effects in LAESI process were revealed when the freeze/thaw solution from the tissue was spiked with  $d_9$ -choline. Spiking at the concentration similar to the value obtained from external calibration did not show any deuterium labeled peak, whereas spiking at higher concentrations did show the peak corresponding to the spiked compound. Therefore, experiments are extended to spiking the tissue at different concentrations.

The tissue was spiked with different concentration of deuterium labeled compounds ( $d_9$ -choline and acetyl- $d_3$ -carnitine) as detailed in Electronic Supplementary Material. The spiked tissue was homogenized by repeated grinding in the presence of liquid nitrogen, and the resulted tissue paste was used for LAESI experiments. The ion count ratios of spiked compound and one the metabolite (reference) that is constant from sample to sample are measured to plot against the concentration of spiked compound. The concentration of the desired metabolite in the tissue (unlabeled) was estimated from the ion count ratio of its protonated molecule with the reference metabolite. Thus, measured tissue concentrations were  $50 \pm 5 \mu\text{g/g}$  for choline and  $170 \pm 20 \mu\text{g/g}$  for acetyl-carnitine. Assuming similar ionization efficiencies for

acetylated and unacetylated analogues the concentrations of acetylcholine and carnitine were also estimated using the calibration curves obtained for  $d_9$ -choline and acetyl- $d_3$ -carnitine, respectively. The tissue concentration of acetylcholine thus measured was  $190 \pm 70 \mu\text{g/g}$  of tissue, and that of carnitine was  $450 \pm 30 \mu\text{g/g}$  of tissue.

### 3.8 Electric organ versus tail muscle tissue

In order to reveal the localization of the identified metabolites in the electric organ tissue, it is important to compare them to the metabolites present in other tissues of the *Torpedo californica*. Thus, we performed LAESI MS experiments on the tail muscle of the same species. The spectrum obtained for this tissue was also dominated by betaine and its quasi-molecular ions ( $m/z$  118, 140, 156, and 257). Ions  $m/z$  74, 83, 90, 96, 102, 112, 114, 116, 132, and 166 were found to be common in both organs but, as expected, there were small variations in the relative abundances of these ions.

Interestingly, the tail muscle tissue did not include many of the important metabolites found in the electric organ. Choline, acetylcholine, carnitine, acetyl carnitine, and trimethyllysine were detected selectively in the electric organ, but were absent or negligible (relative abundance <1.0%) in the tail muscle tissue (Table 2). This confirms

**Table 2** Relative abundances of typical metabolites in the LAESI mass spectra of *Torpedo* electric organ and tail muscle tissue

Metabolite	$m/z$	Relative abundance (%) <sup>a</sup>		
		Electric organ (Jul 2008)	Electric organ (Nov 2004)	Tail muscle tissue (Jul 2008)
Trimethylamine	60	<1	<1	–
Tetramethylammonium	74	17	12	11
Trimethylamine <i>N</i> -oxide or methylethanolamine	76	<1	<1	3
Urea	83	<1	<1	<1
Tetrahydropyridine or dihydromethylpyrrole or cycloalkenyl amine	84	14	13	<1
<i>N</i> -Methylglycine	90	2	3	3
Betaine aldehyde	102	1	1	<1
Choline	104	4	3	<1
Betaine <sup>b</sup>	118	100	100	100
Pipecolic acid	130	19	17	<1
Creatine	132	3	5	5
Acetylcholine	146	6	4	<1
Lysine	147	1	1	–
Carnitine	162	14	15	<1
Dimethyllysine	175	1	1	–
Trimethyllysine	189	20	22	<1
Acetylcarnitine	204	4	3	–
Butyryl-carnitine	232	1	1	–

<sup>a</sup> All spectra were recorded on the same day under identical conditions

<sup>b</sup> Other quasi-molecular ions of betaine were not included in the table

the critical role of these metabolites in the cholinergic function of the electric organ tissue. The high abundance of trimethyllysine, carnitine, and acetyl carnitine in the electric organ is consistent with their role in acetyl choline biosynthesis. The other metabolites found to be selectively present in the electric organ were trimethylamine, pipercolinic acid, lysine, dimethyllysine, and butyrylcarnitine. Furthermore, the LAESI spectra recorded for freshly frozen electric organ tissue (July, 2008) and after low temperature storage (frozen in November, 2004) were similar (Table 2) indicating the stability of the frozen tissue for an extended period with little change in its metabolite composition.

### 3.9 UV-MALDI and ESI analysis

For verification and comparison, we also analyzed the tissue samples with the conventional UV-MALDI and ESI techniques. For UV-MALDI a thin slice of the tissue was placed on the target and was allowed to dry at room temperature. About 2  $\mu$ l of saturated  $\alpha$ -cyano-4-hydroxycinnamic acid (CHCA) (in 50:50 acetonitrile/water with 0.1% TFA) was loaded on the tissue. All the major ions observed in the LAESI spectrum were also seen in the MALDI spectrum but some of the metabolites with low abundance were missing in the latter. In addition, there were some differences in the relative abundances of the ions between the spectra obtained from LAESI and MALDI, which was expected as MALDI necessitated a different sample preparation method and required the use of a matrix. It is known that co-solubility and co-crystallization of the analyte and matrix molecules play a major role in the resulting spectrum. This was clearly evident for the 2,5-dihydroxybenzoic acid (DHB) matrix, as the spectrum did not show any tissue-relevant ions. Indeed, most of the metabolites detected in the electric organ are polar and CHCA is known to be a better matrix choice for the analysis of polar compounds than DHB.

The metabolites of the electric organ tissue were also extracted by water using a freeze/thaw process. The contents were centrifuged and the supernatant was transferred into a fresh tube, which further diluted with equal volume of acetonitrile with 0.1% formic acid. The solution was then infused into our ESI source at a flow rate of 300 nl/min. The ESI spectrum obtained from the water extract was very similar to the LAESI spectrum. No significant changes were noticed in the relative abundances of the ions between the ESI spectrum obtained from the extract and the LAESI spectrum obtained directly from the tissue without any sample preparation. This supports the idea that in LAESI the ions are produced by ESI postionization of the laser ablation plume. It also implies the suitability of the LAESI technique for the rapid analysis of metabolites without altering the native sample environment by sample preparation.

## 4 Conclusions

In most previous direct animal tissue analysis experiments by mass spectrometry, proteins, and related molecules were studied using vacuum UV-MALDI ionization. This method entails time consuming sample preparation steps such as sectioning, occasionally washing, drying, and the application of matrix. These steps can alter the native analyte distributions in the sample; an effect that can be most prominent for small molecules, such as metabolites. Here we report the direct analysis of metabolites from the *Torpedo californica* electric organ tissue by mid-IR LAESI MS. Because LAESI uses the native water of the tissue to couple the laser energy into the sample, it does not require extensive sample preparation or the application of a matrix for analysis. As it only requires placing a small section/portion of the tissue on the target plate before laser ablation in the ambient environment, the method is very rapid and requires minimum handling.

The *Torpedo* electric organ is considered homologous to the mammalian NMJ and hence has been studied in detail as a model for understanding electric synapses. The present report is the first comprehensive investigation of the metabolites in this tissue; hence we have mainly focused on the qualitative aspects of analysis. Ions related to 24 metabolites in the *Torpedo* electric organ tissue were detected with varied ion signals, including the neurotransmitter acetylcholine and its precursor choline, carnitine, acetyl carnitine, and creatine. Most marine fishes accumulate organic osmolytes for protection from osmotic stress. Among the two known osmolytes, betaine and trimethylamine *N*-oxide, we found in the electric organ tissue, the former appeared to be the dominant metabolite. Apart from urea, trimethylamine and the tetramethylammonium ion, we also identified some of the intermediates and precursors of the above metabolites that clarified their biosynthetic pathway. This corroborated the findings of earlier investigations on the enzymes involved in the biosynthesis of these metabolites in the electric organ tissue (Nazarian et al. 2007).

Quantitation of the identified metabolites is essential for the diagnosis of the physiological state of the organism. Wide dynamic range quantitation capabilities of LAESI MS for drug analysis had been demonstrated with standards (Nemes and Vertes 2007). Initial attempts to measure the concentrations of typical metabolites in the electric organ tissue using external calibration method resulted in lower concentration values due to matrix interferences in the tissue and discrimination as well as ion suppression effects in the sampling and ionization steps, respectively. The experiments based on the introduction of deuterium labeled standards into the electrospray also revealed the extent of underreporting absolute concentrations directly from the

tissue. Ultimately, spiking the tissue with deuterated metabolites showed a way to measure the actual quantities of a few important metabolites.

The comparative analysis of the *Torpedo* electric organ and tail muscle tissues clearly revealed the selective role of choline, acetylcholine, carnitine, acetylcarnitine, trimethyllysine metabolites in the former. Reducing the sampling size of the laser ablation in LAESI to dimensions comparable with the electroplaques and ultimately with subcellular features can further our understanding of the NMJ. This requires better focusing of the laser light through aspherical optics or the utilization of a sharpened optical fiber, and improving the sensitivity of the MS detection. Enhanced ionization efficiency and more efficient ion collection in the atmospheric pressure interface can help with the latter.

The metabolomic imaging by LAESI MS has already been demonstrated with 300  $\mu\text{m}$  spatial resolution for plant tissue. Spatial variations in metabolites can reveal the correlations between tissue or cell level differentiation and biological function. For the *Torpedo* electric organ, meaningful imaging requires improving the spatial resolution to  $\sim 5 \mu\text{m}$ .

**Acknowledgments** The authors are grateful for the support of this work by the W. M. Keck Foundation (041904), the National Science Foundation under grant 0719232, and the Research Enhancement Fund of the George Washington University. The opinions, findings, and conclusions or recommendations expressed in this material are those of the authors and do not necessarily reflect the views of the National Science Foundation. The authors thank Peter Nemes (George Washington University) for his help in setting up the LAESI experiments. One of the authors (P. S.) thanks the Director of the Indian Institute of Chemical Technology, Hyderabad, and the Council of Scientific and Industrial Research, India for granting leave.

## References

- Allen, D. L., Roy, R. R., & Edgerton, V. R. (1999). Myonuclear domains in muscle adaptation and disease. *Muscle and Nerve*, *22*, 1350–1360. doi:10.1002/(SICI)1097-4598(199910)22:10<1350::AID-MUS3>3.0.CO;2-8.
- Anderson, D. C., King, S. C., & Parsons, S. M. (1982). Proton gradient linkage to active uptake of  $[3\text{H}]\text{acetylcholine}$  by *Torpedo* electric organ synaptic vesicles. *Biochemistry*, *21*, 3037–3043. doi:10.1021/bi00256a001.
- Bain, M. A., Faull, R., Fornasini, G., et al. (2004). Quantifying trimethylamine and trimethylamine-*N*-oxide in human plasma: interference from endogenous quaternary ammonium compounds. *Analytical Biochemistry*, *334*, 403–405. doi:10.1016/j.ab.2004.07.004.
- Bhuiyan, A. K. M. J., Jackson, S., Turnbull, D. M., et al. (1992). The measurement of carnitine and acyl-carnitines: Application to the investigation of patients with suspected inherited disorders of mitochondrial fatty acid oxidation. *Clinica Chimica Acta*, *207*, 185–204. doi:10.1016/0009-8981(92)90118-A.
- Bino, R. J., Hall, R. D., Fiehn, O., et al. (2004). Potential of metabolomics as a functional genomics tool. *Trends in Plant Science*, *9*, 418–425. doi:10.1016/j.tplants.2004.07.004.
- Brass, E. P. (2002). Pivalate-generating prodrugs and carnitine homeostasis in man. *Pharmacological Reviews*, *54*, 589–598. doi:10.1124/pr.54.4.589.
- Breer, H., Morris, S. J., & Whittaker, V. P. (1978). A structural model of cholinergic synaptic vesicles from the electric organ of *Torpedo marmorata* deduced from density measurements at different osmotic pressures. *European Journal of Biochemistry*, *87*, 453–458. doi:10.1111/j.1432-1033.1978.tb12395.x.
- Bremer, J. (1983). Carnitine—metabolism and functions. *Physiological Reviews*, *63*, 1420–1480.
- Burg, M. B., & Ferraris, J. D. (2008). Intracellular organic osmolytes: Function and regulation. *The Journal of Biological Chemistry*, *283*, 7309–7313. doi:10.1074/jbc.R700042200.
- Caldas, T., Demont-Caulet, N., Ghazi, A., & Richarme, G. (1999). Thermoprotection by glycine betaine and choline. *Microbiology*, *145*, 2543–2548.
- Cody, R. B., Laramée, J. A., & Durst, H. D. (2005). Versatile new ion source for the analysis of materials in open air under ambient conditions. *Analytical Chemistry*, *77*, 2297–2302. doi:10.1021/ac050162j.
- Colmer, T. D., Corradini, F., Cawthray, G. R., & Otte, M. L. (2000). Analysis of dimethylsulphoniopropionate (DMSP), betaines and other organic solutes in plant tissue extracts using HPLC. *Phytochemical Analysis*, *11*, 163–168. doi:10.1002/(SICI)1099-1565(200005/06)11:3<163::AID-PCA501>3.0.CO;2-0.
- Corthay, J., Dunant, Y., Eder, L., & Loctin, F. (1985). Incorporation of acetate into acetylcholine, acetylcarnitine, and amino acids in the *Torpedo* electric organ. *Journal of Neurochemistry*, *45*, 1809–1819. doi:10.1111/j.1471-4159.1985.tb10538.x.
- Dettmer, K., Aronov, P. A., & Hammock, B. D. (2007). Mass spectrometry-based metabolomics. *Mass Spectrometry Reviews*, *26*, 51–78. doi:10.1002/mas.20108.
- Feldberg, W., & Fessard, A. (1942). The cholinergic nature of the nerves to the electric organ of the *Torpedo (Torpedo marmorata)*. *The Journal of Physiology*, *101*, 200–216.
- Ghoshal, A. K., Guo, T., Soukhova, N., & Soldin, S. J. (2005). Rapid measurement of plasma acylcarnitines by liquid chromatography-tandem mass spectrometry without derivatization. *Clinica Chimica Acta*, *358*, 104–112. doi:10.1016/j.cccn.2005.02.011.
- Gillingwater, T. H., & Ribchester, R. R. (2003). The relationship of neuromuscular synapse elimination to synaptic degeneration and pathology: insights from WldS and other mutant mice. *Journal of Neurocytology*, *32*, 863–881. doi:10.1023/B:NEUR.0000020629.51673.f5.
- Goldstein, L., Oppelt, W. W., & Maren, T. H. (1968). Osmotic regulation and urea metabolism in the lemon shark *Negaprion brevirostris*. *The American Journal of Physiology*, *215*, 1493–1497.
- Hanley-Jr., J., Bernasconi, A., Davis, R. et al. (2007). Quantitative analysis of acylcarnitines in plasma, serum and urine by liquid chromatography-tandem mass spectrometry. *Proceedings of the 55th ASMS Conference on Mass Spectrometry and Allied Topics*, Indianapolis, IN, 3–7 June, 2007.
- Hayashi, Y., Katsumoto, Y., Oshige, I., Omori, S., & Yasuda, A. (2007). Comparative study of urea and betaine solutions by dielectric spectroscopy: Liquid structures of a protein denaturant and stabilizer. *The Journal of Physical Chemistry B*, *111*, 11858–11863. doi:10.1021/jp073238j.
- Holm, P. I., Ueland, P. M., Kvalheim, G., & Lien, E. A. (2003). Determination of choline, betaine, and dimethylglycine in plasma by a high-throughput method based on normal-phase chromatography-tandem mass spectrometry. *Clinical Chemistry*, *49*, 286–294. doi:10.1373/49.2.286.

- Israel, M., & Lesbats, B. (1981). Continuous determination by a chemi-luminescent method of acetylcholine-release and compartmentation in *Torpedo* electric organ synaptosomes. *Journal of Neurochemistry*, *37*, 1475–1483. doi:10.1111/j.1471-4159.1981.tb06317.x.
- Jakobs, B. S., & Wanders, R. J. A. (1995). Fatty acid [beta]-oxidation in peroxisomes and mitochondria: The first, unequivocal evidence for the involvement of carnitine in shuttling propionyl-CoA from peroxisomes to mitochondria. *Biochemical and Biophysical Research Communications*, *213*, 1035–1041. doi:10.1006/bbrc.1995.2232.
- Johnson, D. W. (2008). A flow injection electrospray ionization tandem mass spectrometric method for the simultaneous measurement of trimethylamine and trimethylamine *N*-oxide in urine. *Journal of Mass Spectrometry*, *43*, 495–499. doi:10.1002/jms.1339.
- Kamimori, H., Hamashima, Y., & Konishi, M. (1994). Determination of carnitine and saturated-acyl group carnitines in human urine by high-performance liquid chromatography with fluorescence detection. *Analytical Biochemistry*, *218*, 417–424. doi:10.1006/abio.1994.1201.
- Keller-Peck, C. R., Walsh, M. K., Gan, W. B., et al. (2001). Asynchronous synapse elimination in neonatal motor units: Studies using GFP transgenic mice. *Neuron*, *31*, 381–394. doi:10.1016/S0896-6273(01)00383-X.
- Kent, G. C. (1992). *Comparative anatomy of the vertebrates*. St. Louis, MO: Mosby-Year Book.
- Keynes, R. D., Greeff, N. G., & Forster, I. C. (1992). Activation, inactivation and recovery in the sodium channels of the squid giant axon dialysed with different solutions. *Philosophical Transactions of the Royal Society B Biological Sciences*, *337*, 471–484. doi:10.1098/rstb.1992.0122.
- Kistler, J., & Stroud, R. M. (1981). Crystalline arrays of membrane-bound acetylcholine receptor. *Proceedings of the National Academy of Sciences of the United States of America*, *78*, 3678–3682. doi:10.1073/pnas.78.6.3678.
- Kistler, J., Stroud, R. M., Klymkowsky, M. W., Lalancette, R. A., & Fairclough, R. H. (1982). Structure and function of an acetylcholine receptor. *Biophysical Journal*, *37*, 371–383.
- Li, Y., Shrestha, B., & Vertes, A. (2007). Atmospheric pressure molecular imaging by infrared MALDI mass spectrometry. *Analytical Chemistry*, *79*, 523–532. doi:10.1021/ac061577n.
- Li, Y., Shrestha, B., & Vertes, A. (2008). Atmospheric pressure infrared MALDI imaging mass spectrometry for plant metabolomics. *Analytical Chemistry*, *80*, 407–420. doi:10.1021/ac701703f.
- Mardones, C., Vizioli, N., Carducci, C., Rios, A., & Valcarcel, M. (1999). Separation and determination of carnitine and acylcarnitines by capillary electrophoresis with indirect UV detection. *Analytica Chimica Acta*, *382*, 23–31. doi:10.1016/S0003-2670(98)00790-9.
- Mashego, M., Rumbold, K., De Mey, M., et al. (2007). Microbial metabolomics: Past, present and future methodologies. *Biotechnology Letters*, *29*, 1–16. doi:10.1007/s10529-006-9218-0.
- McGarry, J. D., & Brown, N. F. (1997). The mitochondrial carnitine palmitoyltransferase system—From concept to molecular analysis. *European Journal of Biochemistry*, *244*, 1–14. doi:10.1111/j.1432-1033.1997.00001.x.
- Mitra, A. K., McCarthy, M. P., & Stroud, R. M. (1989). Three-dimensional structure of the nicotinic acetylcholine receptor and location of the major associated 43-kD cytoskeletal protein, determined at 22 Å by low dose electron microscopy and X-ray diffraction to 12.5 Å. *The Journal of Cell Biology*, *109*, 755–774. doi:10.1083/jcb.109.2.755. published erratum appears in *The Journal of Cell Biology*, 1989 Oct; 109 (4 Pt 1):1185.
- Morris, D., Bull, G., & Hebb, C. O. (1965). Acetylcholine in the electric organ of *Torpedo*. *Nature*, *207*, 1295. doi:10.1038/2071295a0.
- Nazarian, J., Bouri, K., & Hoffman, E. P. (2005). Intracellular expression profiling by laser capture microdissection: Three novel components of the neuromuscular junction. *Physiological Genomics*, *21*, 70–80. doi:10.1152/physiolgenomics.00227.2004.
- Nazarian, J., Hathout, Y., Vertes, A., & Hoffman, E. P. (2007). The proteome survey of an electricity-generating organ (*Torpedo californica* electric organ). *Proteomics*, *7*, 617–627. doi:10.1002/pmic.200600686.
- Nemes, P., Barton, A. A., Li, Y., & Vertes, A. (2008). Ambient molecular imaging and depth profiling of live tissue by infrared laser ablation electrospray ionization mass spectrometry. *Analytical Chemistry*, *80*, 4575–4582. doi:10.1021/ac8004082.
- Nemes, P., & Vertes, A. (2007). Laser ablation electrospray ionization for atmospheric pressure, in vivo, and imaging mass spectrometry. *Analytical Chemistry*, *79*, 8098–8106. doi:10.1021/ac071181r.
- Park, E. I., & Garrow, T. A. (1999). Interaction between dietary methionine and methyl donor intake on rat liver betaine-homocysteine methyltransferase gene expression and organization of the human gene. *The Journal of Biological Chemistry*, *274*, 7816–7824. doi:10.1074/jbc.274.12.7816.
- Pettegrew, J. W., Levine, J., & McClure, R. J. (2000). Acetyl-L-carnitine physical-chemical, metabolic, and therapeutic properties: Relevance for its mode of action in Alzheimer's disease and geriatric depression. *Molecular Psychiatry*, *5*, 616–632. doi:10.1038/sj.mp.4000805.
- Pierce, C. Y., Barr, J. R., Cody, R. B., et al. (2007). Ambient generation of fatty acid methyl ester ions from bacterial whole cells by direct analysis in real time (DART) mass spectrometry. *Chemical Communications*, *2007*, 807–809. doi:10.1039/b613200f.
- Randall, D. J., & Ip, Y. K. (2006). Ammonia as a respiratory gas in water and air-breathing fishes. *Respiratory Physiology & Neurobiology*, *154*, 216–225. doi:10.1016/j.resp.2006.04.003.
- Randall, D. J., Wood, C. M., Perry, S. F., et al. (1989). Urea excretion as a strategy for survival in a fish living in a very alkaline environment. *Nature*, *337*, 165–166. doi:10.1038/337165a0.
- Rebouche, C. J., & Seim, H. (1998). Carnitine metabolism and its regulation in microorganisms and mammals. *Annual Review of Nutrition*, *18*, 39–61. doi:10.1146/annurev.nutr.18.1.39.
- Rossi, S. G., Vazquez, A. E., Rotundo, R. L., et al. (2000). Local control of acetylcholinesterase gene expression in multinucleated skeletal muscle fibers: Individual nuclei respond to signals from the overlying plasma membrane; Myonuclear domains in muscle adaptation and disease; Postsynaptic signaling of new players at the neuromuscular junction. *The Journal of Neuroscience*, *20*, 919–928.
- Sanes, J. R., & Lichtman, J. W. (1999). Development of the vertebrate neuromuscular junction. *Annual Review of Neuroscience*, *22*, 389–442. doi:10.1146/annurev.neuro.22.1.389.
- Sanes, J. R., & Lichtman, J. W. (2001). Induction, assembly, maturation and maintenance of a postsynaptic apparatus. *Nature Reviews Neuroscience*, *2*, 791–805. doi:10.1038/35097557.
- Shewan, J. M. (1953). The nitrogenous extractives from fresh fish muscle. II-Comparison of several gadoid and elasmobranch species. *Journal of the Science of Food and Agriculture*, *4*, 565. doi:10.1002/jsfa.2740041202.
- Shrestha, B., Li, Y., & Vertes, A. (2008). Rapid analysis of pharmaceuticals and excreted xenobiotic and endogenous metabolites with atmospheric pressure infrared MALDI mass spectrometry. *Metabolomics*, *4*, 297–311. doi:10.1007/s11306-008-0120-8.

- Smutna, M., Vorlova, L., & Svobodova, Z. (2002). Pathobiochemistry of ammonia in the internal environment of fish. *Acta Veterinaria*, *71*, 169–181. Review.
- Stadler, H., & Fuldner, H. H. (1980). Proton NMR detection of acetylcholine status in synaptic vesicles. *Nature*, *286*, 293–294. doi:10.1038/286293a0.
- Steiber, A., Kerner, J., & Hoppel, C. L. (2004). Carnitine: A nutritional, biosynthetic, and functional perspective. *Molecular Aspects of Medicine*, *25*, 455–473. doi:10.1016/j.mam.2004.06.006.
- Takats, Z., Wiseman, J. M., Gologan, B., & Cooks, R. G. (2004). Mass spectrometry sampling under ambient conditions with desorption electrospray ionization. *Science*, *306*, 471–473. doi:10.1126/science.1104404.
- Treberg, J. R., Speers-Roesch, B., Piermarini, P. M., et al. (2006). The accumulation of methylamine counteracting solutes in elasmobranchs with differing levels of urea: A comparison of marine and freshwater species. *The Journal of Experimental Biology*, *209*, 860–870. doi:10.1242/jeb.02055.
- Vaz, F. M., Melegh, B., Bene, J., et al. (2002). Analysis of carnitine biosynthesis metabolites in urine by HPLC-electrospray tandem mass spectrometry. *Clinical Chemistry*, *48*, 826–834.
- Vaz, F. M., Ofman, R., Westinga, K., Back, J. W., & Wanders, R. J. A. (2001). Molecular and biochemical characterization of rat epsilon *N*-trimethyllysine hydroxylase, the first enzyme of carnitine biosynthesis. *The Journal of Biological Chemistry*, *276*, 33512–33517. doi:10.1074/jbc.M105929200.
- Vaz, F. M., & Wanders, R. J. A. (2002). Carnitine biosynthesis in mammals. *The Biochemical Journal*, *361*, 417–429. doi:10.1042/0264-6021:3610417.
- Vekey, K., Telekes, A., & Vertes, A. (2008). *Medical Applications of Mass Spectrometry*. AE Amsterdam, The Netherlands: Elsevier.
- Verhoeven, N. M., Roe, D. S., Kok, R. M., et al. (1998). Phytanic acid and pristanic acid are oxidized by sequential peroxisomal and mitochondrial reactions in cultured fibroblasts. *Journal of Lipid Research*, *39*, 66–74.
- Vertes, A., Nemes, P., Shrestha, B., et al. (2008). Molecular imaging by mid-IR laser ablation mass spectrometry. *Applied Physics A Materials Science & Processing*, *93*, 885–891. doi:10.1007/s00339-008-4750-5.
- Walsh, M. K., & Lichtman, J. W. (2003). In vivo time-lapse imaging of synaptic takeover associated with naturally occurring synapse elimination. *Neuron*, *37*, 67–73. doi:10.1016/S0896-6273(02)01142-X.
- Wood, K. V., Bonham, C. C., Miles, D., et al. (2002). Characterization of betaines using electrospray MS/MS. *Phytochemistry*, *59*, 759–765. doi:10.1016/S0031-9422(02)00049-3.
- Woodhull, A. M. (1973). Ionic blockage of sodium channels in nerve. *The Journal of General Physiology*, *61*, 687–708. doi:10.1085/jgp.61.6.687.
- Yancey, P. H., Clark, M. E., Hand, S. C., Bowlus, R. D., & Somero, G. N. (1982). Living with water stress: Evolution of osmolyte systems. *Science*, *217*, 1214–1222. doi:10.1126/science.7111214.
- Zito, K. (2003). The flip side of synapse elimination. *Neuron*, *37*, 1–2. doi:10.1016/S0896-6273(02)01182-0.